



# Short period forecasting of catchment-scale precipitation. Part II: a water-balance storm model for short-term rainfall and flood forecasting

V. A. Bell, R. J. Moore

## ► To cite this version:

V. A. Bell, R. J. Moore. Short period forecasting of catchment-scale precipitation. Part II: a water-balance storm model for short-term rainfall and flood forecasting. *Hydrology and Earth System Sciences Discussions*, 2000, 4 (4), pp.635-651. hal-00304693

**HAL Id: hal-00304693**

**<https://hal.science/hal-00304693>**

Submitted on 1 Jan 2000

**HAL** is a multi-disciplinary open access archive for the deposit and dissemination of scientific research documents, whether they are published or not. The documents may come from teaching and research institutions in France or abroad, or from public or private research centers.

L'archive ouverte pluridisciplinaire **HAL**, est destinée au dépôt et à la diffusion de documents scientifiques de niveau recherche, publiés ou non, émanant des établissements d'enseignement et de recherche français ou étrangers, des laboratoires publics ou privés.

# Short period forecasting of catchment-scale precipitation. Part II: a water-balance storm model for short-term rainfall and flood forecasting

V.A. Bell and R.J. Moore

Centre for Ecology and Hydrology, Wallingford, Oxfordshire, OX10 8BB, UK  
e-mail for corresponding author: vib@ceh.ac.uk

## Abstract

A simple two-dimensional rainfall model, based on advection and conservation of mass in a vertical cloud column, is investigated for use in short-term rainfall and flood forecasting at the catchment scale under UK conditions. The model is capable of assimilating weather radar, satellite infra-red and surface weather observations, together with forecasts from a mesoscale numerical weather prediction model, to obtain frequently updated forecasts of rainfall fields. Such data assimilation helps compensate for the simplified model dynamics and, taken together, provides a practical real-time forecasting scheme for catchment scale applications. Various ways are explored for using information from a numerical weather prediction model (16.8 km grid) within the higher resolution model (5 km grid). A number of model variants is considered, ranging from simple persistence and advection methods used as a baseline, to different forms of the dynamic rainfall model. Model performance is assessed using data from the Wardon Hill radar in Dorset for two convective events, on 10 June 1993 and 16 July 1995, when thunderstorms occurred over southern Britain. The results show that (i) a simple advection-type forecast may be improved upon by using multiscan radar data in place of data from the lowest scan, and (ii) advected, steady-state predictions from the dynamic model, using “inferred updraughts”, provides the best performance overall. Updraught velocity is inferred at the forecast origin from the last two radar fields, using the mass-balance equation and associated data and is held constant over the forecast period. This inference model proves superior to the buoyancy parameterisation of updraught employed in the original formulation. A selection of the different rainfall forecasts is used as input to a catchment flow forecasting model, the IH PDM (Probability Distributed Moisture) model, to assess their effect on flow forecast accuracy for the 135 km<sup>2</sup> Brue catchment in Somerset.

**Keywords:** rainfall forecasting, flood forecasting, weather radar, satellite, storm model

## Introduction

Simple advection methods based on weather radar provide a practical means of forecasting rainfall fields in real-time out to two to possibly six hours in support of storm and flood warning. The velocity and direction of storm movement may be obtained either from a mesoscale model (Brown *et al.*, 1994) or from weather radar images displaced in time (Moore *et al.*, 1991, 1994a). Forecast fields are then obtained by advecting the current radar image forwards in time according to this trajectory, possibly with some modification. Such forecasts can be formed on a 2 km or 5 km grid as 15 minute rainfall totals and updated every 15 or 30 minutes. These methods, however, fail to perform adequately when there is development of the rainfall field in spatial extent and/or intensity, or when changes in the storm trajectory occur. Whilst the latter may be less important for forecasting over restricted catchment areas, and for the shorter lead times of primary interest to hydrologists, development of the rainfall field can be a major cause of poor advection forecasts, particularly for convective storms.

Attempts to model storm development by inference from time-displaced radar images have led generally to less reliable forecasts (Moore *et al.*, 1991).

A physically-based approach to rainfall forecasting provides an obvious alternative. However, the current generation of mesoscale model (Pedder *et al.*, 2000; Cullen, 1991; Golding, 1990) represents storm dynamics on too coarse a grid to meet the hydrologists' needs – 16.8 km in the case of the Met Office Unified Model – with highly parameterised representations, for example, of convective cloud systems. Even if mesoscale models proved highly reliable at forecasting rainfall amounts their coarse grid scale would fail to meet the hydrological requirement for catchment scale rainfall, at least for the more spatially variable convective storms or for the smaller catchments of particular interest in urban areas. Disaggregation of mesoscale model rainfall to smaller scales provides one possible approach. However, an interesting alternative is to pursue the physics-based approach at a smaller scale and higher level of process representation. An extreme approach would be to employ one of the number of detailed cloud models (Smolarkiewicz

and Clark, 1985) currently developed to support phenomenological studies of precipitation formation. However, in the development of an operational rainfall forecasting model it is important that the complexity of the model formulation is commensurate with the observation data available for assimilation into the model. This argument leads one to consider simple model parameterisations which encapsulate the dominant dynamics affecting precipitation formation.

One such model, which stems from the work of Kessler (1969), Georgakakos and Bras (1984) and Seo and Smith (1992), is the model of French and Krajewski (1994). This model has formed the starting point of the research reported here. It is a simple two-dimensional rainfall model based on the conservation of mass in a vertical cloud column. Since the model is essentially a simple dynamic water balance of the lower atmosphere it has much in common with the conceptual catchment water-balance models familiar to hydrologists working in the land phase of the hydrological cycle. Using a rainfall model parameterisation commensurate with that of a catchment model clearly has much to commend it for the purposes of storm and flood forecasting. Depending on the resolution of the radar data the model is capable of modelling rainfall fields for 1, 2 or 5 km grids and for time intervals of from 5 to 15 minutes, for example. It therefore meets the hydrologist's requirement for forecasts at this fine resolution in space and time.

This paper focusses on exploring alternative forms of the simplified dynamic model for rainfall forecasting. With this in mind, forecasts are obtained by full state reinitialisation of the water balance model using multi-scan radar estimates of liquid water content at each forecast time-origin. This contrasts with the approach of Georgakakos and Bras (1984) and French and Krajewski (1994) who incorporate observation and model uncertainty within a state estimation framework. Consideration of the uncertainty in measurements from radar and sparse hydrometeorological networks, and in the models which employ approximate process dynamics is clearly important. This is particularly so for the small scale and high intermittency of convective rainfall (Georgakakos and Krajewski, 1996). However, there are difficulties in characterising uncertainty adequately. Full state re-initialisation can be a useful approach when uncertainty in the model dynamics is likely to overwhelm that associated with the measurements. The method is simple and allows attention to be focussed on understanding the shortcomings in the model dynamics and how different formulations compare. Casting the model and supporting measurements within a state estimation framework which takes account of their associated uncertainties, and provides estimates of forecast uncertainty, is outside the scope of the present paper.

## Model Derivation

The rainfall forecasting model of French and Krajewski

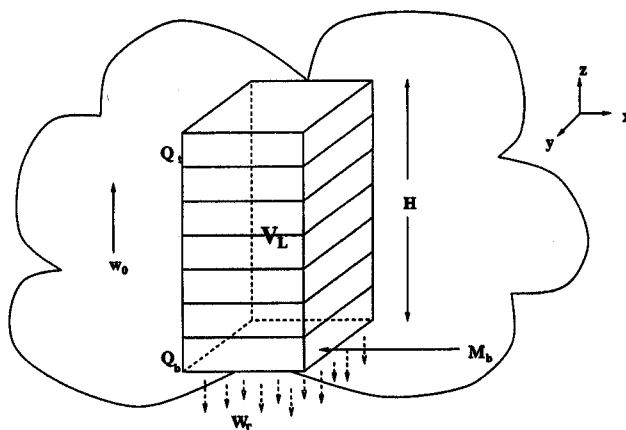


Fig. 1. Schematic of a vertical cloud column in the dynamic rainfall model.

(1994) incorporates both advective and convective dynamics in the form of a two dimensional grid-based horizontal advection scheme coupled with conservation of liquid water in the vertical cloud column associated with each radar grid square. The model is designed primarily for forecasting convective storm rainfall. Figure 1 provides a schematic of a vertical cloud column in the model serving to clarify the notation introduced below.

The underlying model dynamical equation is very similar to the time-dependent moisture budget equation introduced in Part I (Eqn. 1 of Pedder *et al.*, 2000), and takes the form

$$\frac{D}{Dt}(Q + M) = \frac{\partial}{\partial z}(MW_T) \quad (1)$$

where  $Q$  is the saturation water vapour density,  $M$  is liquid water content and  $W_T$  is the terminal velocity of free falling rain in still air;  $D/Dt$  is the total time derivative and  $z$  is the vertical co-ordinate. The quantities  $Q$  and  $M$  are related to specific humidity,  $q$ , and specific liquid water concentration,  $\ell$ , in Part I via  $Q = \rho q$  and  $M = \rho \ell$ , where  $\rho$  is the density of dry air. The term on the right hand side of the equation above can be interpreted as the net surface precipitation rate.

The model dynamical Eqn. 1 is derived from the continuity equations of atmospheric water:

$$\frac{\partial M}{\partial t} + \frac{\partial}{\partial x}(Mu) + \frac{\partial}{\partial y}(Mv) + \frac{\partial}{\partial z}(M(w - W_T)) = \Delta W_c$$

$$\frac{\partial m}{\partial t} + \frac{\partial}{\partial x}(mu) + \frac{\partial}{\partial y}(mv) + \frac{\partial}{\partial z}(mw) = \Delta Q_c - \Delta W_c$$

$$\frac{\partial Q}{\partial t} + \frac{\partial}{\partial x}(Qu) + \frac{\partial}{\partial y}(Qv) + \frac{\partial}{\partial z}(Qw) = -\Delta Q_c$$

$$\frac{\partial \rho}{\partial t} + \frac{\partial}{\partial x}(\rho u) + \frac{\partial}{\partial y}(\rho v) + \frac{\partial}{\partial z}(\rho w) = 0 \quad (2)$$

where  $m$  is cloudwater content and the quantities  $u$ ,  $v$  and  $w$

represent the horizontal and vertical components of velocity in the  $x$ ,  $y$  and  $z$  directions. The terms on the right hand side,  $\Delta W_c$  and  $\Delta Q_c$ , are source terms representing, respectively, the conversion of cloud to rain, and the process of condensation to liquid water vapour.

The system of equations is simplified by considering a moist atmosphere in which on condensation, water vapour is converted to rainwater so efficiently that the cloud phase is unchanged and is uniform in time and space: that is  $Dm/Dt = 0$ . This results in Eqn. 1. Air is assumed to be incompressible and its saturation vapour density is taken to be locally steady and horizontally uniform: that is, the vertical variation of  $Q$  is assumed to be dominant following Kessler (1969).

Using a Lagrangian frame of reference (a frame of reference following the motion of the cloud) and implementing the above assumptions gives

$$\frac{\partial M}{\partial t} = -w \frac{\partial M}{\partial z} + \frac{\partial}{\partial z} (M W_T) - w \frac{\partial Q}{\partial z}. \quad (3)$$

This equation may be integrated over the height of the cloud from the bottom,  $z_b$ , to the top,  $z_t$ , under the assumption of constant vertical velocity,  $w_0$  (necessary because the vertical momentum equation is not included in the model) to give

$$\frac{dV_L}{dt} = w_0(Q_b - Q_t) - (W_T - w_0)M_b \quad (4)$$

where  $V_L \equiv V_L(t)$  is the vertically integrated liquid water content

$$V_L = \int_{z_b}^{z_t} M dz. \quad (5)$$

The suffices  $b$  and  $t$  are used to denote values at the cloud base and top respectively. Equation 4 incorporates the boundary condition of zero rainwater at the cloud top and the assumption that the free fall velocity of water is constant up the height of the cloud i.e.  $\partial W_T / \partial z = 0$ . The equation represents a mass balance equation expressing the change in water content as the difference between the inflow of water between  $z_b$  and  $z_t$ , and the outflow via rain from the cloud base.

## Model Parameterisation

### INTRODUCTION

The mass balance Eqn. 4 may be used as the basis of a rainfall forecasting method by parameterising the unknown variables – the vertically integrated water content  $V_L$ , updraught velocity  $w_0$ , saturation water vapour density  $Q$ , and the terminal velocity of free falling rain in still air  $W_T$  – in terms of quantities measured by weather radar, satellite remote sensors and surface weather stations. The par-

ameterisations outlined below are similar to those employed by French and Krajewski (1994), except for the updraught velocity,  $w_0$ , and the rainwater content at the cloud base,  $M_b$ .

### VERTICALLY INTEGRATED LIQUID WATER CONTENT, $V_L$

Radar measurements of reflectivity,  $Z$ , at different heights in the cloud column are converted to values of rainwater content,  $M$ , using the  $M$ - $Z$  relation

$$M = \frac{\pi \rho_0 \Lambda^3 Z}{720} \quad (6)$$

where  $\rho_0$  is water density and  $\Lambda$  is the drop-size distribution parameter (see Eqn. 8 below). The values of  $M$  are then integrated vertically to give a value of  $V_L$  for the cloud column above each radar grid square.

### TERMINAL RAINFALL VELOCITY, $W_T$

$W_T$  is estimated from the drop-size distribution given by Marshall and Palmer (1948) and an expression for the terminal velocity of rain due to Atlas and Ulbrich (1977), which yield the equation

$$W_T = \Lambda^{-\beta} \frac{\alpha}{6} \Gamma(4 + \beta) = \{M_b / (\pi \rho_0 N_0)\}^{\gamma} \frac{\alpha}{6} \Gamma(4 + \beta) \quad (7)$$

where  $M_b$  is the rainwater content at the cloud base,  $\rho_0$  is water density,  $\Lambda$  and  $N_0$  are dropsizes distribution parameters,  $\Gamma(\cdot)$  is the Gamma function, and  $\alpha$  and  $\gamma = \beta/4$  are dimensionless empirical parameters. Following Marshall and Palmer (1948) the drop-size distribution parameter  $\Lambda$  is related to rainfall rate  $R$  ( $\text{mm h}^{-1}$ ) according to

$$\Lambda = \Lambda_0 R^{-0.21} \quad (8)$$

where  $\Lambda_0$  is regarded as a parameter to be estimated; a typical value for  $\Lambda_0$  is 4.1.

### SATURATED WATER VAPOUR DENSITIES, $Q_b$ AND $Q_t$

The vapour densities are estimated from surface observations of temperature and pressure and satellite-derived cloud top temperature values. Parcel theory is used to calculate values of temperature and pressure at the cloud base and top, from which saturation water vapour densities  $Q_b$  and  $Q_t$  are obtained from

$$Q(z, t) = \frac{r_s(T(z), p(z)) p(z)}{R_d T(z)} = \frac{e e_s(T(z))}{R_d T(z)} \quad (9)$$

applied at the cloud base and top. Here  $T(z)$  is the cloud temperature,  $p(z)$  is the pressure,  $r_s$  is the saturation mixing ratio of air with water,  $R_d$  is the specific gas constant for dry

air,  $e_s(T(z))$  is the saturation vapour pressure and  $\varepsilon$  is a known constant.

#### RAIN WATER CONTENT AT THE CLOUD BASE

Apart from the updraught velocity,  $w_0$ , which is discussed later the final unknown in the mass balance Eqn. 4 is  $M_b$ , the rainwater content at the cloud base. Seo and Smith (1992) estimate  $M(z_b)$  by curve fitting to known values of  $M(z)$  and  $V_L$ , and using the relationship to estimate  $M$  at the cloud base  $z_b$ , taken as the fixed height 2.5 km to avoid ground clutter. They define the cloud depth  $H$  to be the echo-top height above  $z_b$ , and assume it to remain constant over the forecast lead time. For simplicity a linear relationship is assumed between  $V_L$  and  $M_b H$ , at each timestep, of the form

$$M_b = \frac{1}{H} [a(t)V_L(t) + b(t)]. \quad (10)$$

However, scatter plots presented by Seo and Smith suggest that a power law relation might be more appropriate. By contrast, in the work of French and Krajewski (1994) the value of  $M$  at the cloud base is known because  $z_b$  is taken to be the lowest level with non-zero radar reflectivity and  $H$  is the height difference between this and the elevation of the highest non-zero reflectivity. Radar-derived values for  $M$ ,  $H$  and  $V_L$  are used to estimate by regression the parameters  $a$  and  $b$  in Eqn. 10 at each time step, which are then substituted back in place of  $M$ .

The approach taken by French and Krajewski was followed initially, but was found to contribute to errors in rainfall intensity. A scatter plot of  $M_b$  against  $V_L$  failed to reveal a clear relation between the two variables across the field, suggesting that fitting a relation such as (9) across the whole radar field is inappropriate. Instead, the simple power-law relation

$$M_b = \frac{1}{H} a(t) V_L(t)^\mu \quad (11)$$

has been applied to every radar grid square with the value of  $a(t)$  calculated from (10) using radar-derived values of  $M_b$ ,  $V_L$  and  $H$  for each grid square. The resulting field of  $a(t)$  values can then be advected, along with other variables such as temperature and  $V_L$ , so that predicted  $V_L$  can be converted back to rainfall rate for a given forecast lead time. Use of this simple relation has the advantage of removing a certain amount of error from the conversion of  $V_L$  to rainfall rate. Parameter  $\mu$  has been set to unity here; square root and general power law relations provide opportunities for future investigation.

#### SOLUTION TO THE DYNAMIC MODEL

Substituting the parameterisation of the previous sections into Eqn. 4 yields the following ordinary differential

equation (ODE) for the time evolution of the liquid water content in a cloud column:

$$\frac{dV_L}{dt} = AV_L + B(V_L)^{1+\gamma} + S \quad (12)$$

where, in the case  $\mu = 1$ ,

$$V_L = \frac{M_b H}{a} \quad (13)$$

and

$$A = \frac{aw_0}{H} \quad (14)$$

$$B = \frac{-a^{1+\gamma}}{H^{1+\gamma}} (\pi \rho_0 N_0)^{-\gamma} \frac{\alpha}{6} \Gamma(4 + \beta) \quad (15)$$

$$S = w_0(Q_b - Q_i). \quad (16)$$

Note that while the variables  $a$ ,  $w_0$ ,  $Q_b$ ,  $Q_i$  and  $H$  are assumed to be constant over the forecast lead time, they vary in time with each new set of observational data. Hence, forecasts are considered to be full state-initialised predictions.

Equation 12, a nonlinear ODE, may be simplified and solved analytically, or integrated numerically to give the liquid water content at the next time step. Quantities  $A$ ,  $B$  and  $S$  can be considered constants in the solution process and  $\gamma = \beta/4 = 0.1675$ . French and Krajewski chose to solve the ODE analytically via the Gauss-Taylor linearisation technique which facilitates use of the Kalman Filter for real-time state-updating using radar observations. Two further solution schemes are considered here: a "naive" linearisation and a numerical solution of the full nonlinear Eqn. 12.

In the naive linearisation approach an approximate solution is constructed by setting  $\gamma = 0$ , simplifying Eqn. 12 to the linear ODE

$$\frac{dV_L}{dt} = (A + B)V_L + S. \quad (17)$$

This has the solution

$$\ln[(A + B)V_L + S] = (t + k)(A + B) \quad (18)$$

where  $k$  is the constant of integration. With initial condition  $V_L(t)$  at time  $t$  the full solution at time  $t + \Delta t$  may be written as

$$V_L(t + \Delta t) = e^{A^* \Delta t} V_L(t) + (A^*)^{-1} [e^{A^* \Delta t} - 1] S \quad (19)$$

where  $A^* = A + B$ .

For the numerical solution of the full nonlinear Eqn. 12 an adaptive step-size fifth order Runge-Kutta algorithm is used (Press *et al.*, 1989). This algorithm monitors local truncation error to permit adaptive stepsize control and to ensure accuracy.

An assessment of the different solution methods is given in Bell and Moore (1996) which has led to a preference for the simple "naive" linearisation scheme.

## UPDRAUGHT VELOCITY

*Buoyancy parameterisation*

In the French-Krajewski formulation, calculation of the updraught velocity,  $w_0$ , is based on a model of updraught velocity originating from Georgakakos and Bras (1984). This assumes that updraught velocity varies in a piecewise linear fashion, increasing with height above the cloud base, reaching a maximum, then decreasing up to the cloud top where it attains its original value. The piecewise function is such that the vertically averaged updraught velocity,  $w_0$ , occurs at a pressure level  $p_{w_0}$  given by

$$p_{w_0} = 3/4 p(z_b) + 1/4 p(z_t) \quad (20)$$

where  $p(z_b)$  and  $p(z_t)$  are the pressure levels at the cloud base and top respectively. If  $T_m$  is the cloud temperature at this pressure level, assuming pseudoadiabatic ascent, and  $T_{w_0}$  is the corresponding ambient air temperature, then based on an empirical relation of Sulakvelidze (1969)  $w_0$  is obtained as

$$w_0(t) = \varepsilon_0 [c_p (T_m - T_{w_0})]^{1/2} \quad (21)$$

where  $c_p$  is the specific heat of dry air at constant pressure and  $\varepsilon_0$  is a parameter to be estimated. The temperatures  $T_m$  and  $T_{w_0}$  are found using parcel theory.

*Inference method of calculating updraught velocity*

Initial model results suggested that the above buoyancy parameterisation does not lead to realistic values of updraught velocity and an alternative method, related to one investigated by Andrieu *et al.* (1996), was developed. This procedure called the "inference method" uses two successive rainfall fields to calculate the input (and updraught) that would be needed to obtain the current observed  $V_L$  from the last. The analytical solution for the linear form of mass-balance equation (Eqn. 19), considered over the interval  $(t-\Delta t, t)$ , is rearranged to provide a solution for  $w_0$ , given  $V_L$ , so that

$$w_0 \simeq \frac{A^* [V_L(t) - V_L(t-\Delta t)e^{A^*\Delta t}]}{(Q_b - Q_t)(e^{A^*\Delta t} - 1)} \quad (22)$$

with  $A^* = A + B$ . The radar field at time  $t-\Delta t$  is translated using the current advection velocity to coincide as closely as possible with the field at time  $t$ . This formula provides a first approximation only since  $A$ , given by Eqn. 14, itself incorporates  $w_0$  through a term with the form  $(w_0 - W_T)$ . The equation could be solved iteratively to provide a more accurate estimate for  $w_0$ . However, trials suggested that Eqn. 22 gives physically realistic results and was likely to be computationally more efficient than an iterative scheme. An upper bound was placed on estimates of  $w_0$  to avoid unrealistically large values arising when the field advection velocity does not adequately represent the velocity of individual convective cells. This option was seldom invoked, as the magnitude of the field velocity was usually less than  $10 \text{ m s}^{-1}$ .

The updraught velocity parameterisation is clearly an important and difficult issue which is both scale and storm-type dependent. Alternative approaches based on simplifying the vertical momentum equation have been pursued by Lee and Georgakakos (1996) and Nakakita *et al.* (1996).

## CALCULATION OF FORECAST RAINFALL

The method of calculating forecast rainfall uses the following equation for rainfall rate at the cloud base as the estimate of rainfall rate:

$$R = \frac{1}{\rho_0} M_b v_b. \quad (23)$$

Noting that  $M_b v_b = (W_T - w_0) M_b = -(AV_L + BV_L^{1+\gamma})$  yields the following expression for  $R$  in terms of  $V_L$ :

$$R = -\frac{(AV_L + BV_L^{1+\gamma})}{\rho_0}. \quad (24)$$

This eliminates the need to estimate  $M_b$  via Eqn. 11 when calculating rainfall rate,  $R$ , from forecasts of  $V_L$ . It also ensures that the value of  $R$  is consistent with the prediction Eqn. 11. The approximation  $\gamma = 0$  is used here.

## STEADY-STATE FORECASTING WITH UPDRAUGHT

When the linear form of the model (17) is used for rainfall forecasts, precipitation rate,  $R$ , is given by

$$R = -\frac{M_b}{\rho_0} (w_0 - W_T) \equiv -\frac{1}{\rho_0} (A + B) V_L, \quad (25)$$

where updraught,  $w_0$ , is positive upwards and the terminal rain velocity,  $W_T$ , is positive downwards. In the mass-balance model,  $V_L$  varies in time according to

$$\frac{dV_L}{dt} = (A + B) V_L + w_0 (Q_b - Q_t), \quad (26)$$

where  $A$  is a function of  $w_0$ , and  $w_0$  is calculated from (21) at each forecast lead time. Hence, the forecast rainfall rate,  $R$ , is calculated in terms of (i) a varying  $V_L$ , which is initialised at each forecast origin, and (ii) an updraught,  $w_0$ , which is assumed constant over the forecast lead time, but is assigned a new value at each time origin.

A simple forecasting scheme that has proved successful is to keep  $V_L$  constant over the forecast lead time (as for advection or steady-state) and calculate rainfall rate  $R$  according to Eqn. 24 above. Since  $A$  is a function of the constant  $w_0$ , the scheme is not purely steady state, and although the forecasts at various lead times will be the same in intensity, they differ according to the field advection, and have a different intensity to the observed field at the forecast origin. In trials, best results were obtained by calculating a constant  $w_0$  over the forecast lead time from the inference method of Eqn. 22. Use of a vertical momentum equation to

allow for variation in updraught velocity with lead time presents an opportunity for further research.

#### ADVECTION SCHEME

At each time-step the forecast rainfall field is constructed in two stages. First, the current rainfall field is advected horizontally, and then rainfall intensities are adjusted according to the forecast Eqn. 12, which represents growth and decay of the storm. The advection scheme employed here is the HYRAD Advection Scheme developed by Moore *et al.* (1991, 1994a). This scheme searches for the best advection velocity vector by first moving the first field around in whole pixel increments in each direction, corresponding here to velocity increments of  $20 \text{ km h}^{-1}$ . An even finer search using quarter pixel increments (velocity increments of  $5 \text{ km h}^{-1}$ ) is then carried out and finally an interpolation scheme is used to obtain the final best estimate. This finer search makes little difference when lead times are short, but over longer lead times when any overestimate in the field velocity is multiplied up, it can have a significant effect on forecast accuracy. A computationally efficient “log root mean square error” measure of correspondence, between the displaced field at the previous time-step and the current field, is employed in place of the more widely used correlation coefficient.

#### INCORPORATION OF AN AUTOMATIC OPTIMISATION SCHEME

The rainfall forecasting model requires estimation of one or two main parameters:  $\Lambda_0$  in the drop size distribution and, when used,  $\varepsilon_0$  in the updraught velocity Eqn. 21. A third parameter can be invoked either as a rainfall adjustment factor or as an upper bound on the updraught velocity. Initially, the two main parameters were adjusted by hand. The need to compare the performance of different model formulations as objectively as possible and the introduction of a third model parameter prompted the incorporation of an automatic optimisation scheme. This employs a simplex minimisation procedure (Nelder and Mead, 1965) modified to incorporate ideas suggested by Gill *et al.* (1981). The scheme minimises an objective function formed as a measure of the difference between the observed and predicted radar fields. Whilst a range of objective functions is available the one used here is the root mean square error, or rmse, with the error defined as the difference between observed and forecast rainfall in each pixel and the statistic evaluated over all pixels and all time-steps during the period of calibration.

To summarise, the rainfall forecasting model combines an advection scheme with a water mass-balance equation and takes as input radar data, satellite infra-red observations and ground weather station data, with the option of using Mesoscale Model data when available. The formulation

requires estimation of two principal parameters,  $\Lambda_0$  in the drop size distribution and, when used,  $\varepsilon_0$  in the updraught velocity Eqn. 21. All other quantities are estimated from the available observational data.

#### MODEL VARIANTS

An option within the forecasting model permits selection of one of the following methods for calculating cloud column liquid water content at the next lead time or time-step. The options exhibit increasing complexity, a framework designed to examine the behaviour of each model component in turn. Choices are as follows:

(a) **Persistence:** In this, the simplest model variant, the forecast rainfall field is identical to the field observed at the forecast time origin.

(b) **Advection:** This variant is similar to persistence, except that by comparing the current and previous radar fields, a value of average field velocity is inferred which is then used to advect the measured field to produce the new forecast.

(c) **Multiscan advection:** This variant of advection uses radar data from higher scans to determine whether the use of multiscan data can improve on the performance of a simple advection forecast using information from just the lowest radar scan. Investigation of this method was carried out in two ways:

- i) Using the vertically interpolated multiscan radar data, a value for the average rainfall in the cloud column was calculated in the same way that  $V_L$  is calculated – the base of the cloud is detected using the radar data and data above the base are averaged vertically.
- ii) The above method was adapted for use with “raw” radar data which have not been interpolated. Data for all scan elevations above the cloud base (taken to be the lowest scan that detected rainfall) were averaged and the resulting field was advected as in (b) to produce a rainfall forecast.

(d) **Full mass-balance model:** This variant provides for the following three options:

- i) French-Krajewski model formulation incorporating statistical linearisation;
- ii) “Naive linearisation” (assumes  $\gamma = 0$ ); and
- iii) Full nonlinear ODE solved using the adaptive stepsize Runge-Kutta scheme.

Various methods for calculating the model updraught were implemented, including the original buoyancy formulation used by Georgakakos and Bras (1984), the inference method of calculating updraught and estimates obtained from the Mesoscale Model.

(e) **Steady-state forecasts with updraught.** This

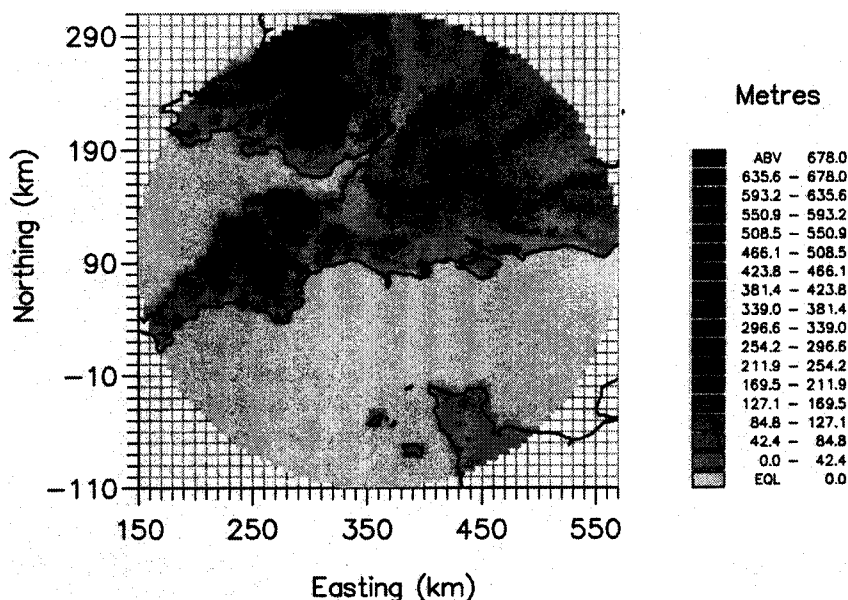


Fig. 2. Variation in surface elevation over the Wardon Hill radar field, as 5 km grid averages derived from a 50 m resolution digital terrain model, used to correct standardised sea level pressures. The Brue catchment is delineated on the map a little north of the centre of the 210 km radius radar circle.

approach was used generally in conjunction with the inference method for calculating updraught velocity.

## Data Requirements

### INTRODUCTION

The model requires data from a multi-scanning weather radar, surface weather stations and satellite imagery, and is also able to use mesoscale model data as an additional source of information.

### WEATHER RADAR DATA

Use of the UK network radar at Wardon Hill in Dorset has meant that the multiscan data have been restricted to 5 km data, on an 84 by 84 grid extending to a range of 210 km, for the four scan elevations of 0.5°, 1.0°, 1.5° and 2.5°. Higher resolution data on a 2 km grid are available only for the lowest scan elevation, out to a range of 76 km, and have not been used here. The maximum scan elevation of 2.5° means that potentially moist parts of the troposphere may not be measured by the radar within a range of about 100 km. Interpolation of the radar data onto a regular three-dimensional grid has been used to reduce problems associated with the limited number and vertical extent of the radar scans, infilling upwards near the radar and downwards at longer range. An extension of the two-dimensional multiquadric surface fitting method, developed by Moore *et al.* (1989, 1994b), to three dimensions has been used for interpolation. Details of the application of this

method are given in Bell and Moore (1996). The resulting regular grid has 10 points spaced 1 km apart in the vertical and 84 by 84 points spaced 5 km apart in the horizontal.

### SURFACE WEATHER STATION DATA

The model requires data for surface air temperature, dew point temperature and pressure from surface weather stations. A set of 11 stations extending over southern England and Wales has been identified to support the study. Data for these synoptic stations are held in the UK Meteorological Office's Synoptic Data Bank for a sampling interval of one hour. For use in the model these data are interpolated onto the same 84 by 84, 5 km grid as the radar data using the two-dimensional multiquadric surface fitting technique.

Pressure data for each of the synoptic stations are held as values standardised to mean sea level. These are first interpolated onto the 84 by 84, 5 km grid and then corrected to correspond to the true elevations using hydrostatic theory (Rogers and Yau, 1989). The surface elevations used are spatially averaged values for the 5 km grid derived from a 50 m digital terrain model for the study area. Figure 2 shows the surface elevation over the radar field. The effect of correcting pressures for elevation has been shown to give only a *very slight* improvement in model performance.

### SATELLITE DATA

The model requires cloud-top temperature data derived from satellite imagery. A primary receiving station, operating at CEH Wallingford, has captured routinely



Meteosat data over the UK for a 30 minute sampling interval since 21 August 1993. Prior to this, data are available from the Met Office archive for a 60 minute sampling interval. The satellite cloud-top temperature data have been interpolated onto the model grid, again using the two-dimensional multiquadric interpolation scheme.

#### MESOSCALE MODEL DATA

The Mesoscale Model (MM) used here is the UK Met Office Unified Model configured on a  $0.15^\circ$  (16.8 km) grid. MM outputs for a 15 minute time interval have been provided by the University of Reading for selected storms. The outputs used here have been limited to surface temperature and pressure data and estimates of updraught velocity; rainfall forecasts have also been used for comparative purposes.

## Assessment of Rainfall Forecasting Model Variants

### INTRODUCTION

The variants of the rainfall forecasting model have been developed and their performance assessed using data for the two periods 9 to 10 June 1993 and 16 July 1995 when thunderstorms occurred over southern Britain. The geographic area for assessment is the area scanned by the Wardon Hill radar in Dorset, and encompassing at about 40 km range the HYREX study catchment of the Brue. The assessment is initially carried out with regard to the quality of the forecast rainfall field, both on a pixel by pixel basis and as catchment averages over the Brue. Later the assessment is extended to consider the quality of flow forecasts derived from using the rainfall forecasts as input to a rainfall-runoff model for the Brue catchment.

### FRAMEWORK FOR ASSESSMENT

The model produces state-initialised forecasts by assimilating data available at each forecast time origin. Each 15 minute time-step in an event was used as the forecast time origin and forecasts constructed for the four lead times 15, 30, 60 and 120 minutes. The following performance measures are calculated on a 5 km grid pooled over the radar field to assess model performance:

- Root mean square error (rmse)
- Root mean square log error (rmsle)
- $R^2$  statistic
- Critical Success Index (CSI).

The "truth" field was taken to be the 5 km grid square values from the lowest level of the interpolated radar field, judged to provide the best radar-derived estimate of rainfall at the ground.

Table 1. Rainfall events used for model assessment.

Event	Start	End	Calibration/ Validation
1	23:57 09/6/93	07:57 10/6/93	Validation
2	15:57 10/6/93	23:57 10/6/93	Calibration
3	10:57 16/7/95	14:57 16/7/95	Calibration
4	14:57 16/7/95	18:57 16/7/95	Validation

The two convective rainfall events, in June 1993 and July 1995, were each split into two periods shown in Table 1 to facilitate independent model calibration and assessment. An initial investigation of the possible presence of solid precipitation in each event, which might adversely affect the model results, suggested this should not be a cause for concern. Calibration and validation were considered necessary for both events because there were differences in the availability of observational data for the two periods. Satellite data for the June 1993 storm were only available for an hourly time-step from the Meteorological Office archive, whereas for the July 1995 event 30 minute interval data were available from the CEH Meteosat receiving station. Secondly, synoptic surface weather observations were not available at the time for the July 1995 event and Mesoscale Model predictions of surface conditions were used instead. However, comparisons between interpolated fields of MM surface data and those derived using the eleven synoptic weather stations suggest that the former provide a more detailed dataset for modelling. The interpolated synoptic dataset provides only a very smoothed field on account of the sparse network of weather stations employed.

Only a minimal level of calibration was needed for each of the model types assessed. The drop-size distribution parameter,  $\Lambda_0$ , was estimated by calibrating the steady-state model at zero lead time to give a near perfect "forecast": the value obtained was used for all model variants where it was needed. The other main parameter,  $\varepsilon_0$ , used in the buoyancy parameterisation of updraught was estimated by minimising the one-step (15 minute) forecast errors; it is used only for the one model variant.

### DESCRIPTION OF RAINFALL EVENTS

A summary of the weather situation for the two storm events used in the assessment follow; the Met Office Daily Weather Summary, the Journal of Meteorology and Weather have been used as sources of information.

**9–10 June 1993:** An anticyclone over Britain receded to the Baltic to be replaced by low pressure. A thunderstorm developed off the Cornish coast late on the 8th and Cornwall experienced a severe thunderstorm during the night. Throughout the morning of the 9th thunderstorms broke out in other parts. The middle of the day was drier and

clearer, but in the evening, as the centre of the low moved over England, a cold front edged into southern England bringing more thunderstorms and rain. The day was very warm and muggy, with light winds. On the 10th a low was centred over the country, with a cold front prevailing. It was warm and humid, with light winds. A thundery airmass encompassed most of the country and thunderstorms were widespread. They were concentrated along the cold frontal zone from North Wales, through the Midlands, to London. An isolated thunderstorm occurred in and around Barnstaple, Devon. In the southwest, rainfall was generally lighter.

16 July 1995: An area of low pressure over the UK moved northwards on the 16th and 17th. Temperatures were close to normal. Showers developed in the southwest and southern counties during the morning, though northern parts remained dry. In the afternoon the showers

became heavier with thunder in places and towards evening the rain moved to more northern areas leaving very little rain in the southwest.

#### RAINFALL FORECAST ASSESSMENT

The relative performance of the different model variants are first assessed on two events used for calibration: events 2 and 3. Using the parameter values obtained from these calibrations, the model is then assessed on events 1 and 4. The performance obtained for calibration and validation are compared below, both across events and between model variants.

##### 9–10 June 1993 event assessment

Table 2 and Fig. 3 summarise the results obtained for each

Table 2. Calibration and validation assessments of different model variants: 9–10 June 1993.

Event number	Start of event	Model variant	Lead time (mins)			
			15	30	60	120
<b>rmse statistic</b>						
2	15:57 10/6/93 Calibration	P	2.215	2.821	3.167	3.520
		A	2.255	2.670	2.927	2.645
		MA	2.276	2.672	2.878	2.568
		D-L	2.094	2.374	<b>2.289</b>	<b>2.097</b>
		D-L- $w_0^{\text{inf}}$	2.263	2.697	3.127	2.830
		SS- $w_0^{\text{inf}}$	<b>1.974</b>	<b>2.259</b>	2.378	2.223
1	23:57 9/6/93 Validation	P	<b>2.250</b>	2.623	2.684	2.810
		A	2.651	2.908	2.994	3.020
		MA	2.499	2.665	2.807	2.785
		D-L	2.261	<b>2.194</b>	<b>2.148</b>	<b>1.746</b>
		D-L- $w_0^{\text{inf}}$	2.451	2.512	2.810	2.891
		SS- $w_0^{\text{inf}}$	2.487	2.732	2.818	2.812
<b>CSI statistic</b>						
2	15:57 10/6/93 Calibration	P	<b>0.695</b>	<b>0.602</b>	<b>0.486</b>	<b>0.380</b>
		A	0.661	0.595	0.480	0.349
		MA	0.657	0.593	0.479	0.345
		D-L	0.613	0.551	0.444	0.324
		D-L- $w_0^{\text{inv}}$	0.555	0.495	0.401	0.276
		SS- $w_0^{\text{inf}}$	0.632	0.569	0.462	0.345
1	23:57 9/6/93 Validation	P	<b>0.485</b>	<b>0.378</b>	<b>0.355</b>	<b>0.255</b>
		A	0.442	0.358	0.321	0.215
		MA	0.442	0.358	0.323	0.217
		D-L	0.354	0.288	0.269	0.179
		D-L- $w_0^{\text{inf}}$	0.323	0.263	0.247	0.158
		SS- $w_0^{\text{inf}}$	0.438	0.357	0.322	0.219

Key: P Persistence

A Advection

MA Multiscan Advection

D-L Dynamic model – linear approximation

D-L- $w_0^{\text{inf}}$  Dynamic model – linear with inferred updraught

SS- $w_0^{\text{inf}}$  Steady state with inferred updraught.

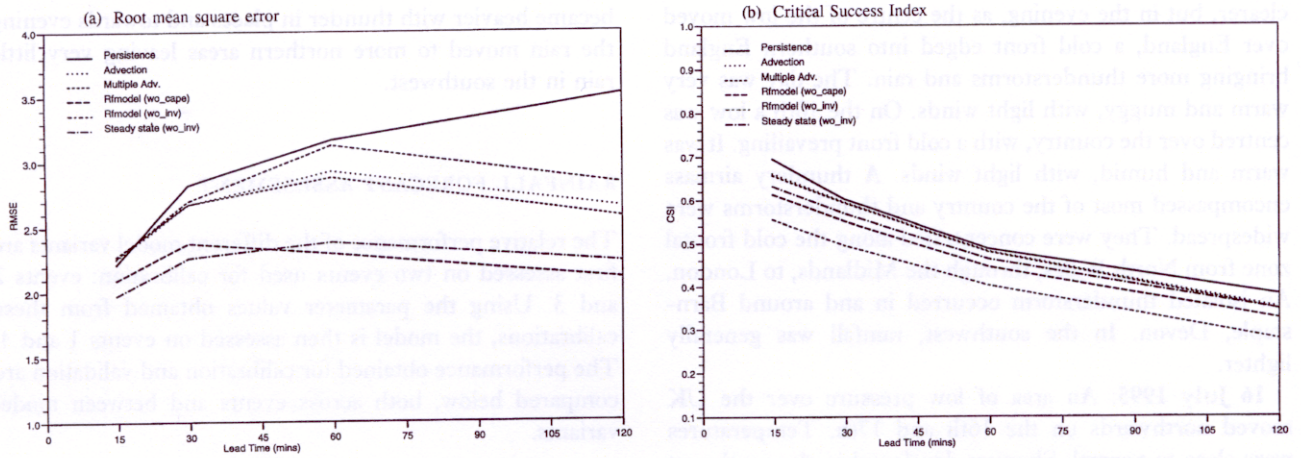
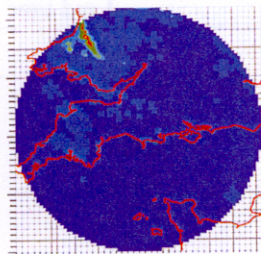
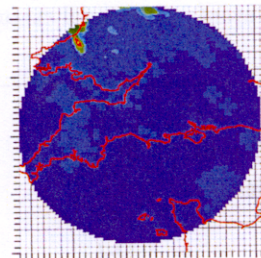


Fig. 3. Variation of forecast accuracy with lead time for the different model variants: 10 June 1993.

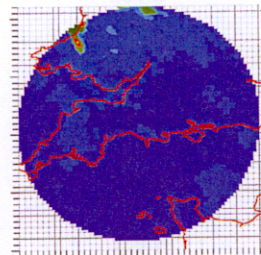
(a) Observed



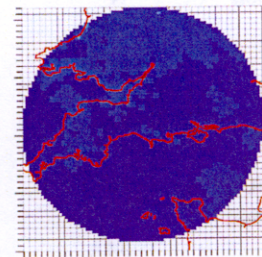
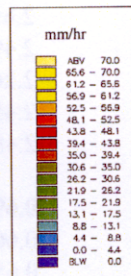
(b) Advection



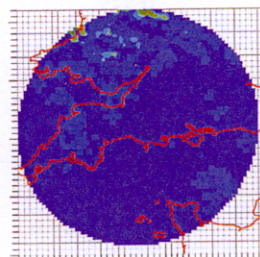
(c) Multiscan Advection



(d) Dynamic model with buoyancy updraught



(d) Dynamic model with inferred updraught



(e) Steady-state with inferred updraught

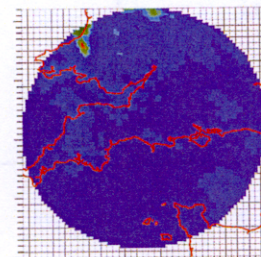


Fig. 4. Comparison of observed and one-hour ahead forecast radar rainfall fields using different model variants: 18:15 10 June 1993.

model variant in terms of rmse and CSI performance measures for the 9–10 June event. Note that whilst Event 1 is a validation event, prior calibration was only involved for the linear dynamic model variant with buoyancy updraught. The results are very different for the two events. Using the rmse criterion, emphasising forecasting rainfall intensity values, the steady-state model with inferred updraught performed best for Event 2. The dynamic model with buoyancy updraught also performs well, but underestimates the updraught resulting in low and smoothed rainfall intensities at longer lead times. This is apparent in Fig. 4 which shows the one-hour ahead forecast rainfall fields for 18:22 10 June 1993 obtained using different model variants. The smoothing seen in Fig. 4 (d) leads to artificially high rmse and rmsle values, an effect noted, and made use of, in Moore *et al.* (1991). The results also demonstrate the advantage of the multiscan advection scheme over the

simple advection scheme through its use of multiscan radar data. The CSI performance measure highlights the performance of forecasting the correct positioning of rainfall, irrespective of its intensity, with a value of unity corresponding to a perfect forecast of the rainfall pattern. For both events used for evaluation the best results were obtained using the very simplest model, persistence. This may reflect fragmentation of the radar images leading to erroneous inferred advection velocities, affecting the more complex models.

#### 16 July 1995 event assessment

Table 3 summarises the results obtained for the event on 16 July 1995 for each model variant in terms of the rmse and CSI performance measures. Figure 5 shows graphically how performance varies with lead time and Fig. 6 compares the

Table 3. Calibration and validation assessments of different model variants: 16 July 1995.

Event number	Start of event	Model variant	Lead time (mins)			
			15	30	60	120
<b>rmse statistic</b>						
3	10:57 16/7/95 Calibration	P	1.151	1.303	1.344	1.307
		A	1.058	1.101	1.256	1.354
		MA	1.044	1.084	1.230	1.319
		D-L	0.909	0.971	1.019	1.023
		D-L- $w_0^{\text{inf}}$	1.085	1.240	1.546	1.648
		SS- $w_0^{\text{inf}}$	0.988	1.027	1.176	1.296
4	14:57 16/7/95 Validation	P	1.143	1.279	1.289	1.286
		A	0.927	1.053	1.254	1.327
		MA	0.913	1.029	1.227	1.291
		D_L	0.825	0.903	0.987	1.013
		D_L- $w_0^{\text{inf}}$	0.931	1.101	1.404	1.600
		SS- $w_0^{\text{inf}}$	0.838	0.934	1.118	1.207
<b>CSI statistic</b>						
3	10:57 16/7/95 Calibration	P	0.535	0.448	0.362	0.296
		A	0.523	0.482	0.377	0.247
		MA	0.522	0.482	0.377	0.248
		D-L	0.354	0.288	0.269	0.179
		D_L- $w_0^{\text{inf}}$	0.468	0.434	0.347	0.214
		SS- $w_0^{\text{inf}}$	0.516	0.477	0.379	0.259
4	14:57 16/7/95 Validation	P	0.525	0.423	0.337	0.228
		A	0.585	0.493	0.375	0.234
		MA	0.583	0.493	0.376	0.236
		D_L	0.465	0.410	0.327	0.221
		D_L- $w_0^{\text{inf}}$	0.425	0.372	0.290	0.175
		SS- $w_0^{\text{inf}}$	0.354	0.288	0.269	0.179

Key: P Persistence  
 A Advection  
 MA Multiscan Advection  
 D-L Dynamic model – linear approximation  
 D-L- $w_0^{\text{inf}}$  Linear Dynamic model with inferred updraught  
 SS- $w_0^{\text{inf}}$  Steady state model with inferred updraught.



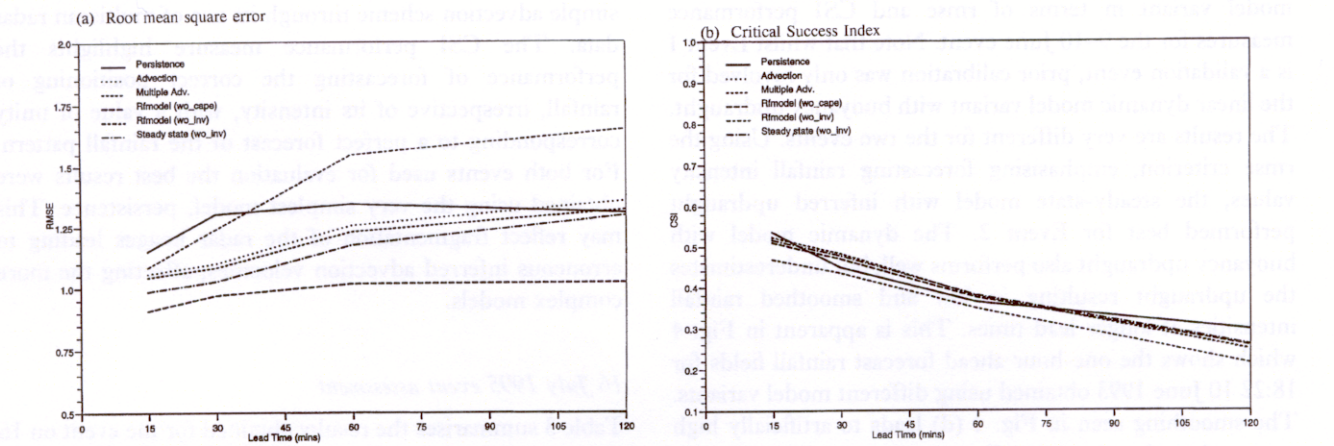


Fig. 5. Variation of forecast accuracy with lead time for the different model variants: 16 July 1995.

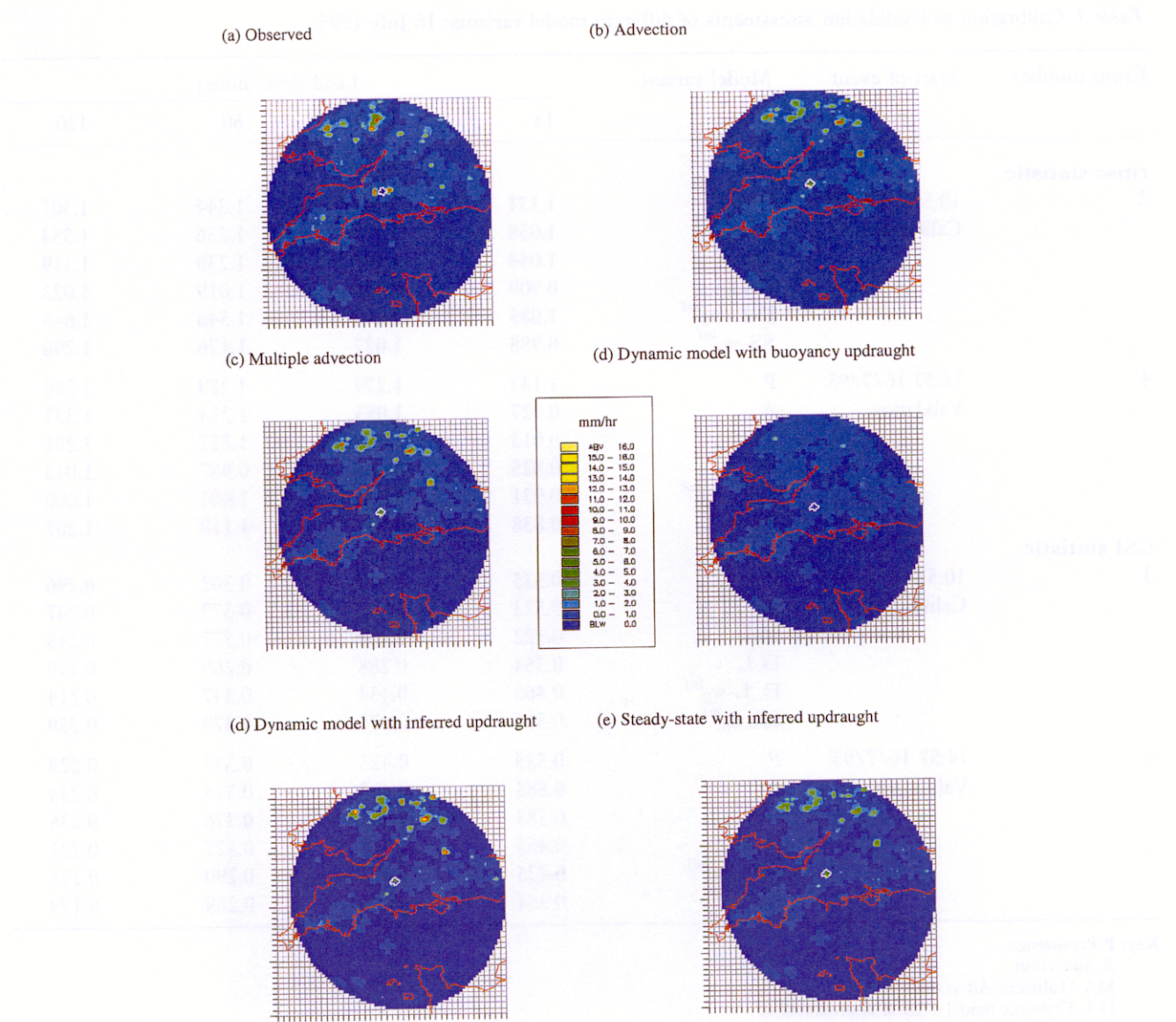


Fig. 6. Comparison of observed and one-hour ahead forecast radar rainfall fields using different model variants: 14:00 16 July 1995.

observed and forecast rainfall fields. Similar conclusions can be drawn from these results as for the June 1993 event. The rmse performance measure suggests that the best variant is the steady-state model with inferred updraught; this discounts the simple linear dynamic model with buoyancy updraught which again produces low, smoothed rainfall fields. The conclusions that can be drawn from the CSI criterion are less clear with no one model outperforming the rest; however, persistence and multiscan advection forecasts perform well.

#### Catchment scale assessment

The rainfall forecasts have so far been assessed at the scale of the radar grid square (5 km) with reference to interpolated radar data as the "truth". For flood forecasting applications, particularly when using lumped rainfall-runoff models, it is important to assess the performance of the rainfall forecasts at the catchment scale. The Brue catchment, as the study area of the HYREX project, has been used here since the dense network of 49 raingauges can be used to obtain a very accurate estimate of the true rainfall over the catchment. Catchment average rainfall has been calculated from the grid-based rainfall forecasts by a simple area-weighted scheme. Figure 7 shows the time-series of catchment average rainfalls derived from the raingauge network, from the rainfall model forecasts and from the Mesoscale Model. The rainfall estimates are seen to vary considerably in both timing and in intensity; the Mesoscale Model forecasts are very low due to problems in the spatial positioning of the rainfall. These catchment-scale rainfall forecasts are assessed later in the context of their use as inputs to a flood forecasting model for the Brue catchment.

#### Overall assessment of model performance

The tables of results and graphs of performance against lead time suggest that the water-balance model with buoyancy

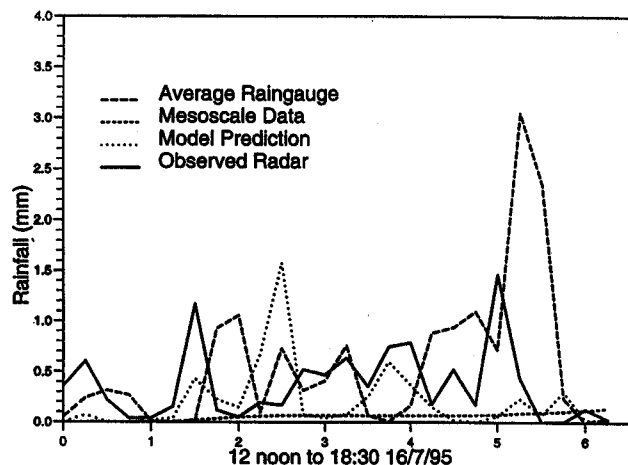


Fig. 7. Comparison of estimates of 15 minute catchment average rainfall totals over the Brue, 12:00 to 18:30 16 July 1995.

updraught is performing quite well. At lead times of over half an hour, all water-balance model variants appear to outperform the simpler persistence and advection forecasts. Unfortunately, this is not due wholly to the models' intended ability to forecast the growth and decay of storms, but is instead due partly to the models' inability to calculate a reasonable value for updraught velocity. Clearly, increasing  $\epsilon_0$  yields higher values of updraught velocity. However, the range of values obtained is very narrow and the updraught across the rain area of the radar field is always much greater than zero. The effect that these very low values of updraught have on model performance is that rainfall rates decrease with increasing lead time, a process which acts as a smoothing effect on the field leading to higher values of rmse, rmsle and  $R^2$ . A similar effect was used by Moore *et al.* (1991) to improve the performance of an advection forecast by smoothing the forecast towards the forecast field average value.

The use of updraught velocity values inferred from two successive radar fields does not appear to result in a smoothing effect and can lead to updraught and down-draught velocities of up to  $10 \text{ m s}^{-1}$ . The resulting rainfall forecasts, however, are less successful than those obtained using other methods. It is possible that the inference method could be improved upon through changes to the field advection scheme, or by invoking a parameter to limit the size of the inferred updraught.

The most successful model formulation appears to be the steady-state scheme with inferred updraught. Experiments have shown that variations on the scheme, such as using the "buoyancy" updraught formulation or using steady-state updraughts (keeping the inferred updraughts stationary with respect to the moving radar field), are less successful.

Use of multiscan radar data in the simple advection scheme – termed "multiscan advection" – rather than data from the lowest scan, has proved very successful. It appears that the use of data from the higher scans to detect rainfall higher in the atmosphere leads to improved forecasts of future rainfall. Similar results were obtained using interpolated radar data and raw radar data without interpolation, in both cases forming an average rainfall across the scans between the cloud base and top. This serves to demonstrate that the success of the multiple advection scheme is not simply an artifact of the multiquadric interpolation.

## Assessment of Rainfall Forecasts for Flood Forecasting

### INTRODUCTION

A second stage of assessment considered how the rainfall forecasts compared when used as input to a flood forecasting model at the catchment scale. The HYREX study catchment of the Brue in Somerset was used for this purpose. The catchment is located about 40 km north of the Wardon

Hill radar and drains an area of  $135 \text{ km}^2$  down to the gauging station at Lovington. Use of this catchment has the benefit that very accurate estimates of catchment average rainfall can be obtained using the HYREX dense network of 49 tipping-bucket raingauges which has been in operation since October 1994. Unfortunately only one event over the period of operation has been judged suitable for use in assessment, in being convective in nature and causing a flow response within the catchment. This event occurred on 16 July 1995 causing a minor flow peak of  $1.3 \text{ m}^3 \text{ s}^{-1}$  at 04:00 17 July.

The PDM (Probability Distributed Moisture) model was used as the rainfall-runoff model in the assessment. This is a simple conceptual catchment model which is used operationally for flood forecasting in various parts of the UK and overseas; it has also recently been used to assess various types of radar rainfall forecast for flood forecasting (Moore *et al.*, 1993; Austin and Moore, 1996). The PDM model employs a probability-distributed soil moisture store (Moore, 1985) to partition rainfall into direct and subsurface runoff which are subsequently translated to the catchment outlet via either linear or nonlinear storage routing elements (Moore, 1999). PDM model forecasts are updated to take account of up-to-the-minute flow measurements using an empirical state-correction technique described in Moore (1999); ARMA error prediction was also considered as an updating technique but was found to be less robust.

#### FRAMEWORK FOR ASSESSMENT

The PDM model was calibrated to the Brue catchment using both catchment average radar and gauge rainfall data for periods of record not containing the event of interest. Various two to three month periods were used for calibration and  $R^2$  values greater than 0.9 were obtained in simulation mode. The sets of calibration parameters were validated on different events before they were used for the assessment event.

A selection of forecast rainfall fields has been used as input to the catchment model to assess their effect on flow forecast accuracy. Five time origins on 16 July were selected before the flow peak at 13:00, 15:00, 17:00, 19:00 and 21:00. At each time origin a two hour rainfall forecast from the forecasting model was used as input, and an eight hour flow forecast generated. The  $R^2$  and rmse performance statistics were calculated over each hour period for each forecast method assessed. The different rainfall forecasts evaluated included persistence, advection, zero rainfall and variants of the mass-balance model.

The PDM was run using the set of calibration parameters derived for radar data, so as to be consistent with the radar-derived rainfall forecasts. To accommodate the build-up of soil moisture deficit over a summer of very little rain, the PDM was initialised on the previous month, June 1995, and then evaluated over July. Figure 8 shows the observed and

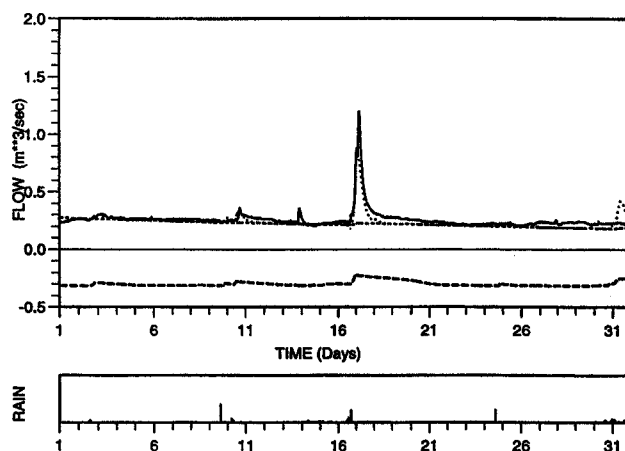


Fig. 8. Observed (continuous line) and simulated (dotted line) flow for the Brue catchment, July 1995. (Dashed line: modelled baseflow; lower dashed line: soil moisture deficit on a dimensionless scale; lower graph: rainfall hyetograph.).

simulated flow in the Brue for July 1995; the concurrent rainfall is shown in the lower graph. The  $R^2$  performance statistic for the month of July is 0.68 in simulation mode, improved to 0.996 after state-updating for the one-step (15 minute) ahead forecast.

#### ASSESSMENT OF RAINFALL AND FLOW FORECASTS

Figure 9 shows the five fixed-origin forecasts for four different types of rainfall forecast. Figure 9(a) shows the flow forecast that would have resulted from perfect foreknowledge of rainfall, using the measured catchment average radar rainfall values. This provides a benchmark against which the next three hydrographs might be compared: these derive from assuming zero rainfall 9(b), advection 9(c) and water-balance model with inferred updraught 9(d). The assumption of zero rainfall after the forecast time origin, as shown in 9(b), does not lead necessarily to poor flow forecasts. Flow forecasts from the first two time origins either miss the flow event completely or underestimate it, but forecasts from time origins that start later in the event are affected less badly because the model is able to use earlier measured rainfall data. Figures 9(c) and (d) look very similar and show the two best forecast results, with the advection forecast depicted in (c) proving the best overall performer. Identical catchment rainfall totals over the Brue were obtained from using simple and multiscan advection forecasts which lead to identical flow forecasts for each model. The water-balance model with inferred updraught Fig. 9(d) performed third best; a surprising result from a model which performed poorly at forecasting the development of the whole radar field. Finally, the other good performer was the steady-state model with inferred

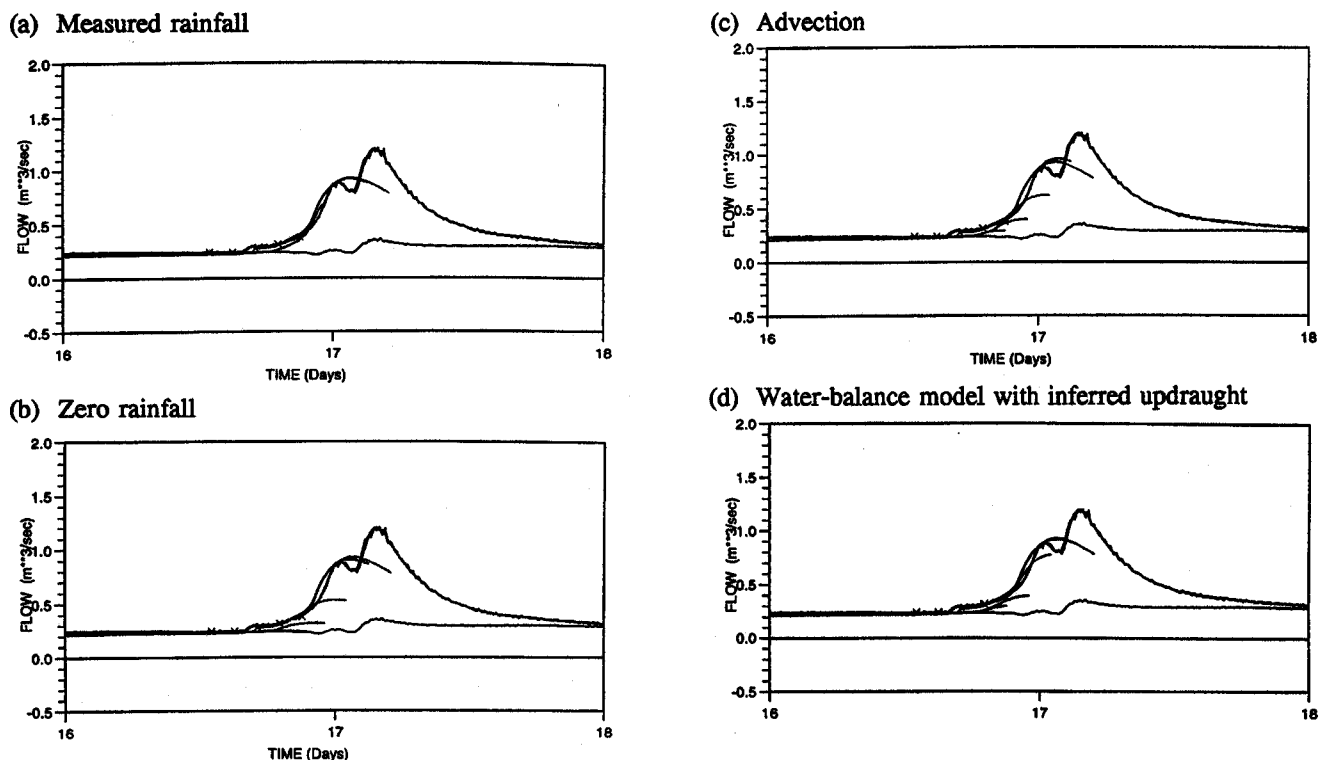


Fig. 9. Fixed-origin flow forecasts resulting from the use of different rainfall forecasts.

updraught, omitted because the result was almost indistinguishable from 9(d).

Table 4 summarises the  $R^2$  performance criteria for the eight different types of rainfall forecast, for each of the five time origins. As the hydrographs in Fig. 9 show, most flow forecasts fail to predict the double-peak in the observed hydrograph. The river network configuration is dominated by the convergence of two main rivers whose different response times is thought to be responsible for the double peak. A simple distributed flow forecasting model might be more successful at representing this behaviour. Note that the apparent good performance of the Mesoscale Model rainfall forecasts for the final time origin is spurious, with

even the measured rainfall failing to reproduce the double-peak. It is most likely an artifact of the unchanging low level of rainfall predicted by the MM over the Brue.

In summary, the flow forecasting results obtained for the convective event on 16 July 1995 over the Brue catchment suggest that at the start of the event the use of a simple rainfall forecast, instead of the assumption of zero forecast rainfall, can improve flow prediction. Towards the end of the storm, there is less benefit to be gained from the use of rainfall forecasts rather than a zero future rainfall assumption. The best overall flow forecasts are obtained using a simple advection rainfall forecast; the water-balance model using inferred updraught and the

Table 4.  $R^2$  performance statistic for flow forecasts out to 8 hours made from five time origins using different rainfall forecasts.

Rainfall forecast	13:00	15:00	17:00	19:00	20:00
Measured radar	0.088	0.788	0.955	0.888	0.556
Zero rainfall	-1.19	-0.18	0.495	0.884	0.556
Persistence	-0.66	0.194	0.975	0.884	0.556
Advection	-0.121	0.442	0.737	0.883	0.556
Mesoscale rainfall	-1.06	-0.045	0.554	0.883	0.556
Multiscan advection	-0.121	0.442	0.734	0.883	0.556
Mass balance: inferred $w_0$	-0.192	0.385	0.945	0.892	0.558
Steady state: inferred $w_0$	-0.737	0.295	0.900	0.887	0.564



steady-state model also with inferred updraught are also good performers.

## Summary and Conclusions

A simple two-dimensional rainfall forecasting model originally developed in the USA for use with 12 elevation scan radar data (French and Krajewski, 1994) has been converted for use with 4 elevation scan UK weather radar data and satellite imagery. The model incorporates components representing field advection and simple convective processes in a vertical cloud column and is capable of assimilating weather radar, satellite infra-red and surface weather observations, together with forecasts from a mesoscale numerical weather prediction model.

A number of model variants has been developed and evaluated over southwest Britain for two convective storms in June 1993 and July 1995. Alongside a linearised form of the mass-balance model, two further variants have been evaluated: (i) a mass-balance model with inferred updraught, and (ii) an advected steady-state model with inferred updraught. The latter model proved most successful for forecasting rainfall fields up to two hours ahead, and usually performed better than the simpler advection or persistence models.

This study has also explored whether some of the apparent success of the mass-balance models is due to the use of the extra information contained in the multiscan radar data. The results suggest that a simple advection forecast might be improved upon by using multiscan radar data in place of data from the lowest radar scan. Some of the success of the more complex model formulations may be due to their use of data from higher radar scans to give an indication of water droplets higher in the atmosphere that may contribute to rainfall on the ground in the near future.

The rainfall forecasting model is capable of assimilating forecasts from a mesoscale model. These data have been used to provide an estimate of updraught velocity, to provide a more detailed field of surface temperature and pressure than can be obtained from the synoptic weather station network, and to provide another type of rainfall forecast for use as input to a flow forecasting model. Further scope exists for investigating the use of Mesoscale Model data to support high resolution short-term rainfall forecasting.

Forecast rainfall fields from a convective storm in July 1995 have been integrated to form 15 minute catchment average rainfall totals over the 135 km<sup>2</sup> Brue catchment in Somerset. The forecasts have been used as input to a catchment flow forecasting model, the IH PDM (Probability Distributed Moisture) model, to assess their effect on flow forecast accuracy. The results for this one storm, whilst clearly not conclusive, suggest that rainfall forecasts are particularly useful at the start of a storm for forecasting future river flows. The best flow forecasts are obtained using

an advection rainfall forecast, with the mass-balance and steady-state models incorporating inferred updraught coming a close second. The failure of the lumped rainfall-runoff model to reproduce the double-peaked hydrograph has highlighted the possible benefit of using a distributed flow forecasting model for the Brue catchment. Such a model will also be able to take advantage of the distributed nature of the radar-derived rainfall forecasts.

## Acknowledgements

This work forms a contribution to the HYREX project "Methods for short-period precipitation and flow forecasting incorporating radar data" funded by the Natural Environment Research Council under its Special Topic research programme, with infrastructure support provided by the NRA (now the Environment Agency), MAFF, the Meteorological Office and the Water Services Association. Additional support has come from the CEC Environment Programme through the project "Storms, Floods and Radar Hydrology". The study forms part of a collaborative project with the Joint Centre for Mesoscale Meteorology (JCMM), University of Reading, who provided the surface weather observation and radiosonde data, accessed from the Met Office's Synoptic Data Bank, together with the Mesoscale Model output. Dawn Carrington is thanked for her earlier contributions to the project. Finally, thanks are due to Dr Mark French of the Department of Civil Engineering, University of Louisville, USA for the computer code to an initial form of the model and useful discussions during a visit to the Institute of Hydrology in 1993. Shared experiences, of the model applied in France, with Hervé Andrieu, LCPC, Nantes as a partner in the CEC project are gratefully acknowledged.

## References

- Andrieu, H., French, M.N., Thauvin, V. and Krajewski, W.F., 1996. Adaption and application of a quantitative rainfall forecasting model in a mountainous region. *J. Hydrol.*, **184**, 243–259.
- Atlas, D. and Ulbrich, C.W., 1977. Path- and area-integrated rainfall measurement by microwave attenuation in the 1–3 cm band. *J. Appl. Meteorol.*, **16**, 1322–1331.
- Austin, R.M. and Moore, R.J., 1996. Evaluation of radar rainfall forecasts in real-time flood forecasting models. *Quaderni di Idronomia Montana*, **16**, (Special Issue, Proc. Workshop on "Integrating Radar Estimates of Rainfall in Real-Time Flood Forecasting"), 19–28.
- Bell, V.A. and Moore, R.J., 1996. *A water-balance storm model for short-term rainfall forecasting using weather radar, satellite infra-red and surface weather observations: an assessment over south west Britain*. Contract report to MAFF, Document HYREX 1/IH/2, Version 1.0, 60 pp.
- Brown, R., Newcomb, P.D., Cheung-Lee, J. and Ryall, G., 1994. Development and evaluation of the forecast step of the FRONTIERS short-term precipitation forecasting system. *J. Hydrol.*, **158**, 79–105.
- Cullen, M.J.P., 1991. The unified forecast/climate model. *Meteorol. Mag.*, **122**, 81–94.

- French, M.N. and Krajewski, W.F., 1994. A model for real-time quantitative rainfall forecasting using remote sensing. Part 1 Formulation. *Water Resour. Res.*, 30, 1075–1083.
- Georgakakos, K.P. and Krajewski, W.F., 1996. Statistical-microphysical causes of rainfall variability in the tropics. *J. Geophys. Res.*, 101, 26, 165–26, 180.
- Gill, P.E., Murray, W. and Wright, M.H., 1981. *Practical Optimisation*. Academic Press.
- Golding, B.W., 1990. The Meteorological Office mesoscale model. *Meteorol. Mag.*, 119, 81–86.
- Georgakakos, K.P. and Bras, R.L., 1984. A hydrologically useful station precipitation model, Part I, Formulation. *Water Resour. Res.*, 20, 1585–1596.
- Kessler, E., 1969. On the distribution and continuity of water substance in atmospheric circulation, *Meteorol. Monogr.*, 10, 86 pp.
- Lee, T.H. and Georgakakos, K.P., 1996. Operational rainfall prediction on meso- $\gamma$  scales for hydrologic applications. *Water Resour. Res.*, 32, 987–1003.
- Marshall, J.S. and Palmer, W.M.K., 1948. The distribution of raindrops with size, *J. Meteorol.*, 5, 165–166.
- Moore, R.J., 1985. The probability-distributed principle and runoff production at point and basin scales. *Hydrol. Sci. J.*, 30, 273–297.
- Moore, R.J., 1999. Real-time flood forecasting systems: perspectives and prospects. In *Floods and Landslides: Integrated Risk Assessment*, R. Casale and C. Margottini (Eds.), Chapter 11, 147–189, Springer.
- Moore, R.J., Watson, B.C., Jones, D.A. and Black, K.B., 1989. *London weather radar local calibration study: final report*. Contract report to the National Rivers Authority Thames Region, 85 pp, Institute of Hydrology, Wallingford, UK.
- Moore, R.J., Hotchkiss, D.S., Jones, D.A. and Black, K.B., 1991. *London Weather Radar Local Rainfall Forecasting Study: Final Report*. Contract Report to NRA Thames Region, 129 pp, (November 1992 update), Institute of Hydrology, Wallingford, UK.
- Moore, R.J., Austin, R.M. and Carrington, D.S., 1993. *Evaluation of FRONTIERS and Local Radar Rainfall Forecasts for use in Flood Forecasting Models*. R&D Note 225, Research Contractor: Institute of Hydrology, National Rivers Authority, 156 pp.
- Moore, R.J., Hotchkiss, D.S., Jones, D.A. and Black, K.B., 1994a. Local rainfall forecasting using weather radar: the London Case Study. In: *Advances in Radar Hydrology*, M.E. Almeida-Teixeira, R. Fantechi, R. Moore and V.M. Silva (Eds.), European Commission, EUR 14334 EN, 235–241.
- Moore, R.J., May, B.C., Jones, D.A. and Black, K.B., 1994b. Local calibration of weather radar over London. In: *Advances in Radar Hydrology*, M.E. Almeida-Teixeira, R. Fantechi, R. Moore and V.M. Silva (Eds.), European Commission, EUR 14334 EN, 186–195.
- Nakakita, E., Ikebuchi, S., Nakamura, T., Kanmuri, M., Okuda, M., Yamaji, A. and Takasao, T., 1996. Short-term rainfall prediction method using a volume scanning radar and grid point value data from numerical weather prediction. *J. Geophys. Res.*, 101, 26, 181–26, 197.
- Nelder, J.A. and Mead, R., 1965. A simplex method for function minimisation, *Computer Journal*, 7, 308–313.
- Pedder, M.A., Haile, M. and Thorpe, A.J., 2000. Short period forecasting of catchment-scale precipitation. Part I: the role of Numerical Weather Prediction. HYREX Special Issue, *Hydrol. Earth System Sci.*, 4, 627–633.
- Press, W.H., Flannery, B.P., Teukolsky, S.A. and Vetterling, W.T., 1989. *Numerical Recipes: The Art of Scientific Computing (FORTRAN Version)*. Cambridge University Press, 702 pp.
- Rogers, R.R. and Yau, M.K., 1989. *A short course in cloud physics*. Pergamon, New York, 3rd ed., 293 pp.
- Seo, D.J. and Smith, J.A., 1992. Radar-based short-term rainfall prediction, *J. Hydrol.*, 131, 341–367.
- Smolarkiewicz, P.K. and Clark, T.L., 1985. Numerical simulation of the evolution of a three dimensional field of cumulus clouds. Part I: Model description, comparison with observations and sensitivity studies. *J. Atmos. Sci.*, 42, 502–522.
- Sulakvelidze, G.K., 1969. *Rainstorms and hail*. Israel Program for Scientific Translations, Jerusalem.